

This article was downloaded by: [Tomsk State University of Control Systems and Radio]

On: 23 February 2013, At: 07:35

Publisher: Taylor & Francis

Informa Ltd Registered in England and Wales Registered Number: 1072954

Registered office: Mortimer House, 37-41 Mortimer Street, London W1T 3JH, UK



## Molecular Crystals and Liquid Crystals

Publication details, including instructions for authors and subscription information:

<http://www.tandfonline.com/loi/gmcl16>

### Studies of Hole-Trap Distribution and Valence-Band Structure in Anthracene

Z. Burshtein<sup>a</sup> & A. Many<sup>a</sup>

<sup>a</sup> The Racah Institute of Physics, The Hebrew University of Jerusalem, Jerusalem, Israel

Version of record first published: 21 Mar 2007.

To cite this article: Z. Burshtein & A. Many (1974): Studies of Hole-Trap Distribution and Valence-Band Structure in Anthracene, *Molecular Crystals and Liquid Crystals*, 25:1-2, 31-44

To link to this article: <http://dx.doi.org/10.1080/15421407408083402>

PLEASE SCROLL DOWN FOR ARTICLE

Full terms and conditions of use: <http://www.tandfonline.com/page/terms-and-conditions>

This article may be used for research, teaching, and private study purposes. Any substantial or systematic reproduction, redistribution, reselling, loan, sub-licensing, systematic supply, or distribution in any form to anyone is expressly forbidden.

The publisher does not give any warranty express or implied or make any representation that the contents will be complete or accurate or up to date. The accuracy of any instructions, formulae, and drug doses should be independently verified with primary sources. The publisher shall not be liable for any loss, actions, claims, proceedings, demand, or costs or damages

whatsoever or howsoever caused arising directly or indirectly in connection with or arising out of the use of this material.

# Studies of Hole-Trap Distribution and Valence-Band Structure in Anthracene<sup>†</sup>

Z. BURSHTEIN and A. MANY

*The Racah Institute of Physics  
The Hebrew University of Jerusalem  
Jerusalem, Israel*

*(Received July 25, 1973)*

Measurements are reported of the spectral yield and other characteristics of the photocurrent arising from photoexcitation of holes out of bulk traps into the valence band of anthracene. Vapour-grown crystals were found to contain two main sets of hole traps: an essentially discrete shallow set, about 1 eV above the valence-band edge and present with a density of  $\sim 10^{11} \text{ cm}^{-3}$ , and a deeper set lying 1.8 - 2.1 eV above the valence-band edge with a density of  $\sim 5 \times 10^{12} \text{ cm}^{-3}$ . The trap density in meltgrown samples is one to two orders of magnitude lower.

The spectral yield of the photocurrent arising from photoexcitation of trapped holes injected by an ohmic contact revealed the following information. A well-defined peak near the photocurrent threshold ( $\sim 1 \text{ eV}$ ) indicates clearly the presence of a narrow conducting sub-band at the top of the valence band of anthracene. The sub-band is less than 0.2 eV in width and is separated from a broad continuum of lower conducting states by at most 0.2 eV. This structure is similar to that observed previously for the conduction band of anthracene except that vibronic splittings of the narrow sub-band are not apparent here. Also, de-trapping of holes by photo-generated triplet excitons is much weaker than in the case of electron traps.

## INTRODUCTION

In previous work<sup>1</sup> measurements of photocurrents arising from optical excitation of trapped electrons in anthracene were used to study the energy distribu-

<sup>†</sup> The research reported herein has been sponsored in part by the European Research Office, U.S. Army, London, England.

tion of the traps on the one hand and the conduction-band structure on the other. It was shown that the spectral response of the photocurrent yield in the photon-energy range 0.9 - 3.3 eV originated from photoexcitation of electrons from a discrete set of traps filled by electron injection. The traps were 0.95 eV deep and present with a density of about  $10^{13} \text{ cm}^{-3}$ . Detrapping was found to occur by direct photoexcitation into the conduction band at long wavelengths and by the interaction of occupied traps with optically generated triplet and singlet excitons at shorter wavelengths. In the long wavelength region (0.9 - 1.7 eV), the spectral yield of the photocurrent revealed steps and peaks separated by energy intervals ranging between 0.03 and 0.08 eV. This suggested that the structure of the lower portion of the anthracene conduction band arises from the interaction of one or possibly more narrow electronic bands with vibronic modes in that energy range. At higher photon energies (1.7 - 2.7 eV), where de-trapping occurs predominantly by photo-generated triplet excitons, many additional vibronic splittings of the triplet state were resolved.

In the present paper we describe similar measurements carried out on the same type of anthracene crystals but involving optical transitions between *hole* traps and the *valence band*. The vapour-grown samples were found to contain two main sets of traps: a shallow set lying about 1 eV above the valence-band edge and having a density of  $\sim 10^{11} \text{ cm}^{-3}$ , and a deep set lying in the range 1.8 - 2.3 eV above the valence-band edge and present with a density of  $\sim 5 \times 10^{12} \text{ cm}^{-3}$ . The shallow set could be fairly accurately characterized. It is essentially discrete in energy, which is a valuable advantage in the study of the valence-band structure. As in the case of electron traps, the hole trap density in the melt-grown crystals was found to be considerably lower ( $\sim 10^{11} \text{ cm}^{-3}$ ).

The spectral photocurrent yield arising from the photoexcitation of trapped holes reveals a well defined, narrow peak near the photocurrent threshold (around the photon energy of 1.15 eV). This peak is much more pronounced than in the analogous case of electron photoexcitation.<sup>1</sup> It indicates clearly the presence of a narrow conducting sub-band at the top of the anthracene valence-band. The sub-band is less than 0.2 eV in width and is separated from the much broader continuum of lower conducting states by at most 0.2 eV. The structure here is similar to that observed for the conduction band<sup>1</sup> except that no vibronic splittings of the sub-band are apparent.

Contrary to the case of electron de-trapping,<sup>1</sup> triplet excitons do not play any detectable role in the optical de-trapping of holes. The spectral yield curve in the triplet photon-energy range (1.7 - 2.8 eV) shows no structure characteristics of the triplet absorption spectrum. It arises, as at lower photon energies, predominantly from direct photoexcitation. Under these conditions the spectral yield curve can provide more meaningful information on the structure of the continuum of conducting states below the narrow sub-band.

## EXPERIMENTAL

The measurements were carried out on anthracene crystals grown in this laboratory from the vapour phase and from the melt. In the former case the samples were thin platelets ( $10 - 100 \mu$  in thickness), oriented parallel to the (a,b) plane, as directly obtained from the growth batch. In the latter case, the samples were cut out from the ingot by a wire saw and subsequently polished to the desired thickness ( $0.3 - 0.5 \text{ mm}$ ). Their orientation was parallel to the (a,c) plane.

The samples were enclosed in sandwich-type cells, one electrode being a transparent conducting glass, the other a hole-injecting contact. The latter electrode consisted of CuI and was prepared as follows. A copper layer of about  $1000 \text{ \AA}$  in thickness and  $0.1 \text{ cm}^2$  in area was evaporated onto one face of the sample. Subsequently, this face was exposed to iodine vapour for about 5 minutes. The CuI electrodes so obtained were found to be very effective as hole injectors. They had the additional advantage of being practically transparent. This property has not been made use of, however, illumination of the sample having been made through the conducting-glass electrode.

The sample holder, the current and photocurrent measuring circuit, and the optical system were as described previously.<sup>1</sup>

## RESULTS AND DISCUSSION

In the dark, appreciable currents were observed only when the applied dc voltage was such as to make the CuI electrode positive. This polarity will be referred to as the "forward" polarity and corresponds to hole injection from the CuI electrode. As in the case of electron injection into anthracene,<sup>1</sup> the injected *hole* current can be enhanced by illumination. Also *after* a forward voltage has been applied, a photocurrent is observed in the reverse polarity ("reverse photocurrent") which decays with time of illumination. Both characteristics are associated with the photoexcitation of holes from traps filled up by injection. (In the case of the reverse photocurrent, the hole traps were filled by the prior application of the forward voltage.)

We describe first the measurements obtained on vapour-grown anthracene platelets. In Figure 1 the forward and reverse photocurrents are plotted as a function of the *forward* (injecting) voltage on a log-log scale. The sample was illuminated with light of wavelength  $0.75 \mu$  and of intensity of  $1.4 \times 10^{14}$  photon/cm<sup>2</sup> sec. The forward photocurrent is in effect a photo-enhanced space-charge-limited current,<sup>1</sup> photoexcitation of holes out of traps produced by the illumination acting to increase the ratio of free to trapped charge. The reverse photocurrent corresponding to a given *forward* voltage was obtained as follows. The

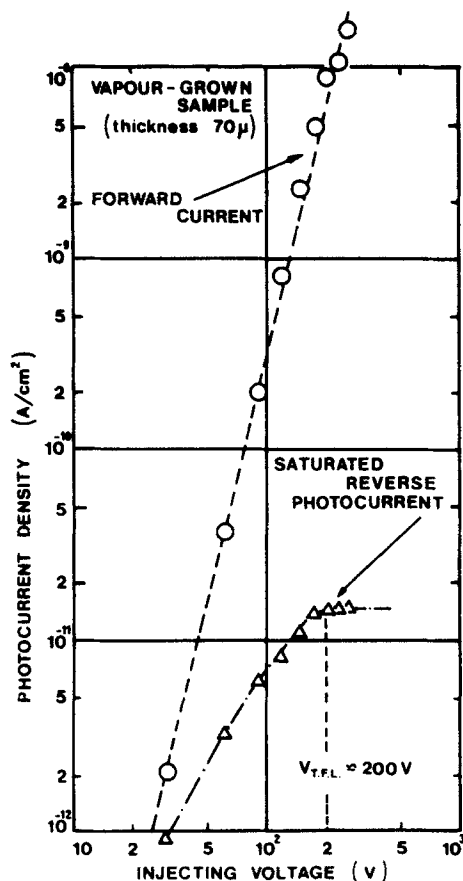


FIGURE 1 Log-log plots of forward and saturated reverse photocurrent as functions of forward injecting voltage. Illumination at wavelength  $\lambda = 0.75\mu$  with intensity  $F = 1.4 \times 10^{14}$  photons/cm<sup>2</sup> · sec. (Vapour-grown sample.)

forward voltage is first applied for a few minutes (in the dark) to allow for a fraction of the traps to be filled by the injected holes. The voltage polarity is then reversed and the initial photocurrent following illumination is measured. (The reverse voltage is made sufficiently large so as to prevent re-trapping of photoexcited holes—see next Figure.) The reverse photocurrent measured in this manner is seen to saturate for an injecting voltage about 200 V. This voltage represents the trap-filled limit  $V_{TFL}$  for which the injected space charge is sufficient to fill up all the available hole traps. To within a factor of two, or so, the density  $N_t$  of these traps is given by<sup>1</sup>  $(2\epsilon_0\kappa/qL^2)V_{TFL}$ , where  $\epsilon_0$  is the permittivity of free space,  $\kappa$  the relative dielectric constant and  $L$  the sample's

thickness. Using the value  $\kappa = 4$ ,  $L = 70 \mu$  and  $V_{TFL} \approx 200 \text{ V}$ , one obtains  $N_t \approx 10^{13} \text{ cm}^{-3}$ .

The variation of the reverse photocurrent with reverse voltage is shown in Figure 2 for the same sample and under the same illumination. The forward injecting voltage applied prior to the measurement had been 100 V. The photocurrent at zero reverse voltage, and also at small negative voltages, is due to the polarization field set up by the prior injection. The curve is seen to start out linearly and to saturate at higher voltages. The voltage  $V_c$  at which the transition from linear to saturation conditions occurs is about 20 V. This means that at this voltage, the hole Schubweg  $\mu_p(V_c/L)\tau_t$ , where  $\mu_p$  is the hole mobility and  $\tau_t$  the hole trapping time, is comparable to the sample's thickness  $L$ . Using the value<sup>2</sup> of  $0.5 \text{ cm}^2/\text{V}\cdot\text{sec}$  for  $\mu_p$ , one obtains an estimate of  $5 \mu\text{sec}$  for the trapping time.

The reverse photocurrent density plotted in Figure 1 corresponds to the *saturated* photocurrent, as obtained under a reverse voltage of 60 V. Its magnitude is given by<sup>1</sup>

$$J_s = \frac{1}{2} q L (dp_t/dt), \quad (1)$$

where  $dp_t/dt$  is the rate of photoexcitation out of traps. The photocurrent decays with time as the hole traps are being emptied by photoexcitation and field sweep-out. The decay (or bleaching) characteristics of the photocurrent will be discussed below.

A good idea about the energy distribution of the hole traps was obtained by the following experiment. The saturated reverse photocurrent at a given wavelength  $\lambda$  was first measured directly following the prior application of a fixed forward voltage. The light intensity used was kept sufficiently low so that no significant bleaching occurred during the brief measurement time. Next the

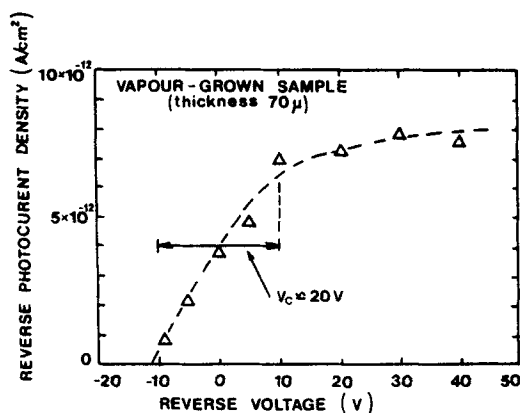


FIGURE 2 Reverse photocurrent as function of reverse voltage. Illumination conditions same as in Figure 1. Forward injecting voltage applied prior to measurement 100V.

sample was bleached by intense and prolonged illumination at wavelengths  $\lambda > 1.1\mu$  such that all traps shallower than 1.14 eV (the photon energy corresponding to  $1.1\mu$ ) were emptied out. The saturated reverse photocurrent at the wavelength  $\lambda$  was then re-measured under identical conditions. The ratio of the reverse photocurrents after and before bleaching is plotted in Figure 3 as a function of wavelength  $\lambda$ . This ratio is a measure of the relative contribution to the reverse photocurrent of traps that are deeper than 1.14 eV. This contribution is seen to be small up to a photon energy of about 1.6 eV ( $\lambda \approx 0.8\mu$ ), indicating that the energy range of 1.1 - 1.6 eV above the valence band is practically free of traps. At higher energies, the trap density increases up to about 2.3 eV ( $\lambda = 0.6\mu$ ). The results thus indicate the presence of two sets of traps, a shallow set less than 1.14 eV above the valence band and a deeper set in the range 1.6 - 2.3 eV above the valence band.

Estimates of the densities of traps responsible for the reverse photocurrent are provided by the bleaching characteristics of the reverse photocurrent. In Figure 4 the time decay of the saturated reverse photocurrent is plotted on a semi-log scale for bleaching at  $\lambda = 1.1\mu$ . At this wavelength only the shallow set of traps can be photoexcited. Moreover, the traps are being emptied by direct optical excitation only, since no triplet excitons are photogenerated by the light.<sup>1</sup> For such direct photoexcitation, the reverse photocurrent decay should be exponential if the traps are discrete in energy.<sup>1</sup> It is given by

$$\begin{aligned} J &= J_0 \exp(-FA\lambda t), \\ J_0 &= \frac{1}{2}qLp_t(0)FA\lambda, \end{aligned} \quad (2)$$

where  $p_t(0)$  is the initial density of trapped holes,  $F$  the photon flux, and  $A\lambda$  the cross section for photoexcitation of a trapped hole into the valence band at bleaching light of wavelength  $\lambda$ . Since  $FA\lambda$  is given by the decay constant of the bleaching curve and  $J_0$  by the initial value of the reverse photocurrent, both  $A\lambda$

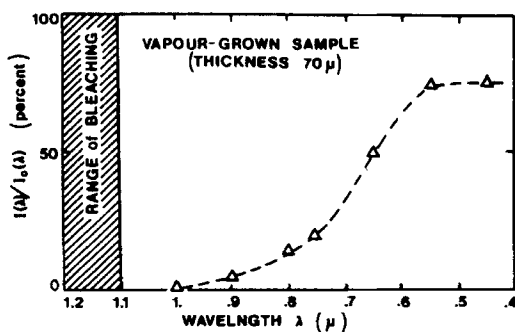


FIGURE 3 Spectral dependence of ratio  $I(\lambda)/I_0(\lambda)$  of saturated reverse photocurrent after and before prolonged bleaching at long wavelengths ( $\geq 1.1\mu$ ).



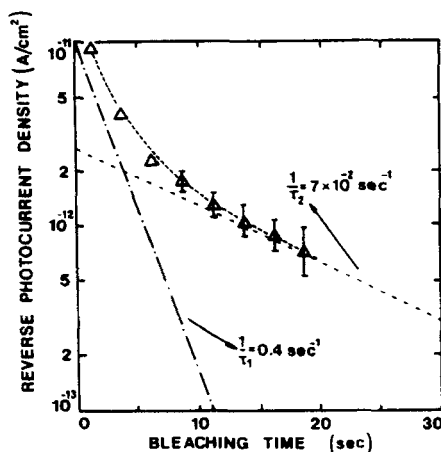


FIGURE 4 Semi-log plot of reverse photocurrent as function of bleaching time. Bleaching at  $\lambda = 1.1\mu$  with intensity  $F = 5.6 \times 10^{14}$  photons/cm<sup>2</sup>·sec. Resolution of curve into two exponential components depicted by dashed straight lines.

and  $p_t(0)$  can be determined. Obviously the decay curve in Figure 4 is not exponential, indicating that the shallow set of traps is not strictly discrete. However, the decay curve can be resolved into two exponentials, as depicted in Figure 4 by the dashed straight lines. On the assumption that each exponential corresponds to a discrete sub-set of traps, one can apply eq.(2) to derive the trap density and cross section of each sub-set. The values so obtained are  $p_t(0) \approx 5 \times 10^{10}$  cm<sup>-3</sup> and  $A_\lambda \approx 10^{-15}$  cm<sup>2</sup> for one set and  $p_t(0) \approx 2 \times 10^{11}$  cm<sup>-3</sup> and  $A_\lambda \approx 2 \times 10^{-16}$  cm<sup>2</sup> for the other set. The forward injecting voltage was sufficiently large so as to fill up all the traps. Hence their values of  $p_t(0)$  represent the trap densities of the two sub-sets. The average density of the shallow traps is about  $10^{11}$  cm<sup>-3</sup> with an average cross section for photoexcitation at  $\lambda = 1.1\mu$  of about  $5 \times 10^{-16}$  cm<sup>2</sup>.

The reverse-photocurrent decay for bleaching with light of  $\lambda = 0.55\mu$  is shown in Figure 5. The triangles represent measurements after prolonged bleaching at  $\lambda = 1.1\mu$  so that only the deep set of traps is involved. The decay is nearly exponential, yielding for the density of deep traps the value of about  $5 \times 10^{12}$  cm<sup>-3</sup>. On the assumption that de-trapping of holes by triplet excitons is not significant (see below), one obtains for the cross section for direct photoexcitation by light of  $0.55\mu$  the value of  $5 \times 10^{-17}$  cm<sup>2</sup>. Also shown in Figure 5 is the decay curve obtained without prior bleaching at  $1.1\mu$  (circles). The fast initial component originates from the shallow set of traps, which are now of course also photoexcited by the  $\lambda = 0.55\mu$  light.

An estimate for the depth of the shallow set of traps has been obtained by thermal bleaching experiments. A forward injecting voltage is applied as before,

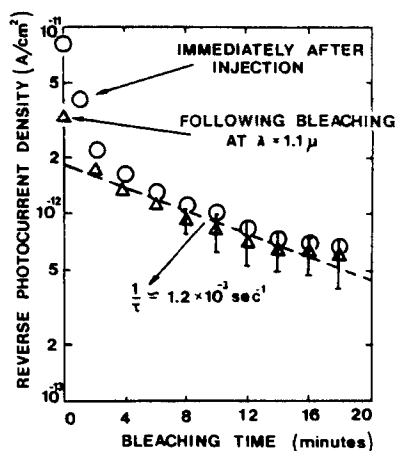


FIGURE 5 Bleaching curves immediately after injection (circles) and following prolonged bleaching at  $1.1\mu$  (triangles). Illumination at  $\lambda = 0.55\mu$  with intensity  $F = 3.2 \times 10^{13}$  photons/cm<sup>2</sup> · sec.

and the saturated reverse photocurrent at  $\lambda = 1.1\mu$  is measured at different times following the prior injection. The sample is kept in the dark except during the brief measurement intervals. Also the light intensity used was sufficiently low so that optical bleaching was negligible. Since the reverse photocurrent is directly proportional to the density of trapped holes, its decay with time represents the rate of reduction in the density of trapped holes due to *thermal* emission into the valence band. In Figure 6 the time decay of the ratio  $I(t)/I(0)$  ( $=p_t(t)/p_t(0)$ ) of the saturated reverse photocurrent at time  $t$  to that immediately following injection is plotted on a semi-log scale for two ambient temperatures. In both cases the decay is seen to be exponential, indicating that essentially only one discrete set of traps is involved. The slope of the straight line at each temperature  $T$  represents the reciprocal of the thermal emission time constant  $\tau_e$ , which is given by<sup>3</sup>

$$\tau_e = (v_T \sigma N_v)^{-1} \exp(\Delta E_t / kT); \quad (4)$$

here  $v_T$  is the average thermal velocity of a free hole,  $\sigma$  the hole capture cross section of the traps,  $N_v$  the effective density of states in the valence band, and  $\Delta E_t$  the depth of the traps. Taking for anthracene,<sup>4</sup>  $V_T = 3 \times 10^5$  cm/sec and <sup>5</sup>  $N_v = 7 \times 10^{21}$  cm<sup>-3</sup> one obtains from the data in Figure 6 that  $\Delta E_t \approx 1.1$  eV and  $\sigma \approx 5 \times 10^{-14}$  cm<sup>2</sup>. This value of  $\Delta E_t$  corresponds very well to the photon energy 1.15 eV of the light used in measuring the reverse photocurrent ( $\lambda = 1.1\mu$ ).

The thermal bleaching of the deep set of traps is not feasible since the emission time constants would be impractically long.

Having obtained a characterization of the hole-trap distribution we now

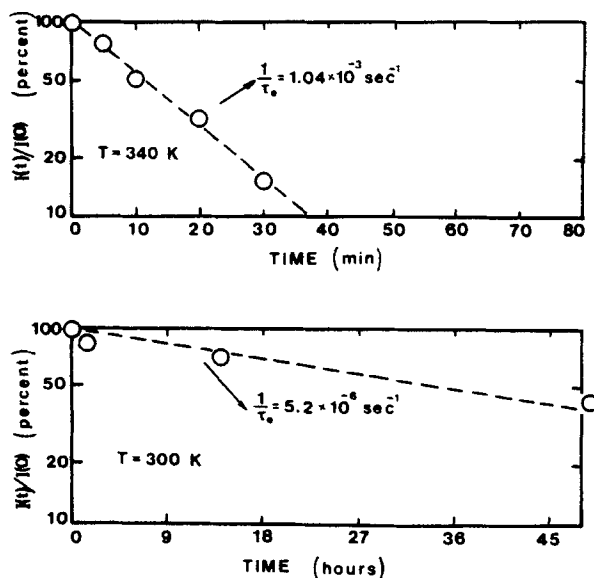


FIGURE 6 Semi-log plots of thermal bleaching curves at two temperatures. Ordinate represents  $I(t)/I(0)$ , where  $I(0)$  and  $I(t)$  are, respectively, the saturated reverse photocurrents immediately after injection and after sample has been kept in the dark for time  $t$ .

proceed to measurements of the spectral response of the reverse photocurrent. In Figure 7 the photocurrent yield (electrons per incident photon), as measured directly following injection (circles) and after prolonged bleaching at  $\lambda = 1.1\mu$  (triangles), is plotted against photon energy. The latter plot shows negligible photocurrent at photon energies less than about 1.6eV, indicating once again (see Figure 3) that the energy range between the shallow and deep traps (1.2 - 1.6 eV) is practically free of traps. Moreover, the thermal bleaching measurements described above (Figure 6) show that the shallow set of traps is essentially a discrete one. Thus for photon energies less than about 1.6eV, the unbleached spectral yield curve (circles) arises from photoexcitation of holes from a nearly discrete set of traps into various levels of the valence band. The most significant feature of the yield curve in this energy range is the occurrence right after the threshold energy of a well defined, narrow ( $\sim 0.2\text{eV}$ ) peak at photon energies around 1.13eV. This indicates the presence of a narrow conducting sub-band at the top of the valence band of anthracene, well separated from the continuum of lower conducting states. The presence of this sub-band is apparent also, even if in a less pronounced manner, in the yield curve obtained after the shallow traps have been bleached out (triangles). In this case the peak corresponds to photoexcitation from the deep set of traps (which is probably more spread out in energy) into the narrow sub-band.

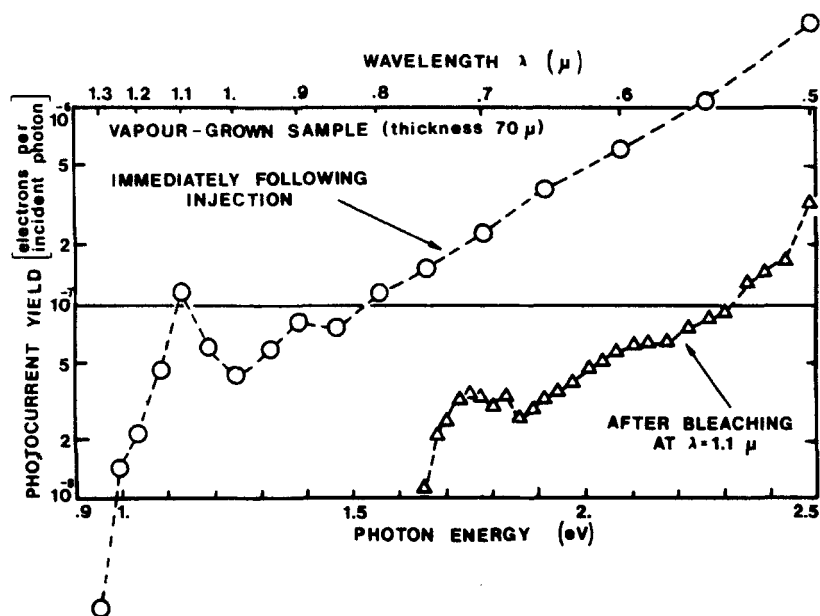


FIGURE 7 Spectral response of reverse-photocurrent yield immediately following injection (circles) and after the shallow traps have been bleached out by prolonged illumination at  $\lambda = 1.1\mu$  (triangles).

The photocurrent yield in the photon energy range of  $\sim 1.2 - 1.6$  eV must be a result of direct optical excitation from the shallow set of traps into a continuum of states below the narrow sub-bands. At higher photon energies, optical excitation from both sets of traps takes place. Here as well, the optical excitation is probably mostly direct since, contrary to the case of *electron* photoexcitation into the conduction band of anthracene,<sup>1</sup> no structure in the yield curve characteristic of de-trapping by triplet excitons is apparent in the photon-energy range of 1.7 - 2.8 eV.

We describe now a similar set of measurements carried out on melt-grown samples. In Figure 8 the dark and photo-enhanced hole currents are plotted on a log-log scale as functions of the injecting voltage. The same plot is obtained during the increasing and decreasing direction of the applied voltage. This indicates that most of the traps controlling the dark current are fairly shallow, their thermal-emission time-constant being less than a few minutes (the time between successive measurements).

In Figure 9 the reverse photocurrent (following a fixed injecting voltage) is plotted against the reverse voltage. An analysis similar to that above (Figure 2) leads to a value of  $5 \mu\text{sec}$  for the trapping time  $\tau_t$ .

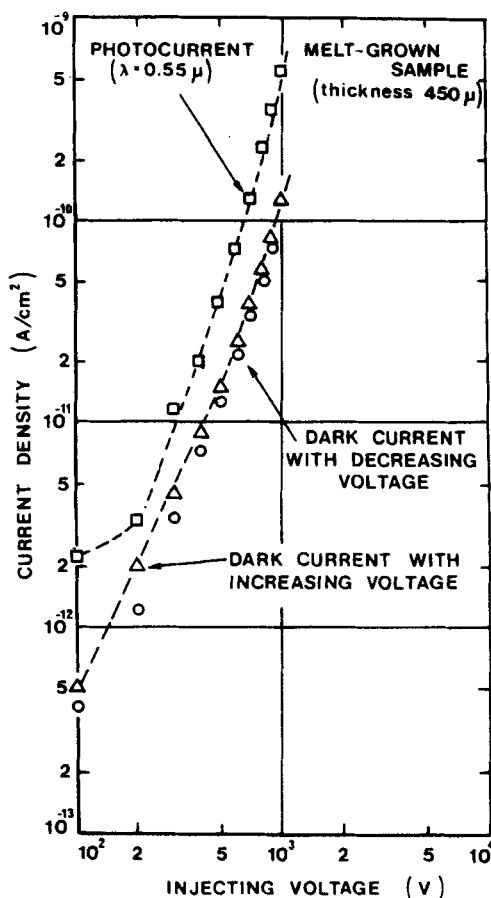


FIGURE 8 Log-log plots of dark and photo-enhanced ( $\lambda = 0.55 \mu$ ) current as function of forward injecting voltage. (Melt-grown sample.)

The reverse photocurrent is too low to permit meaningful measurements of the bleaching characteristics. All that can be said is that the trap densities in the melt-grown crystals are between one and two orders of magnitude lower than those in the vapour-grown platelets. The spectral yield of the photo-enhanced space-charge-limited current (i.e., under a forward injecting voltage) could, however, be measured and is displayed in Figure 10. The barely resolved peak (this time at photon energies around  $1.4eV$ ) is very likely here, as well, a result of optical excitation from a set of hole traps  $1.2 - 1.4eV$  deep into the narrow sub-band of the valence band.

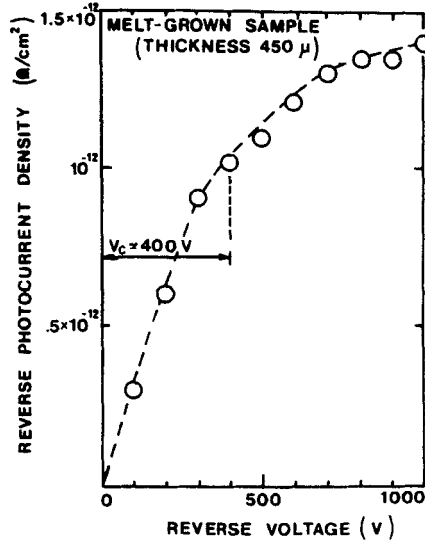


FIGURE 9 Reverse photocurrent as function of reverse voltage. Illumination at  $\lambda = 0.55 \mu$ , intensity  $F = 3.5 \times 10^{13}$  photons/ $\text{cm}^2 \cdot \text{sec}$ . Forward injecting voltage applied prior to measurement 1000V.

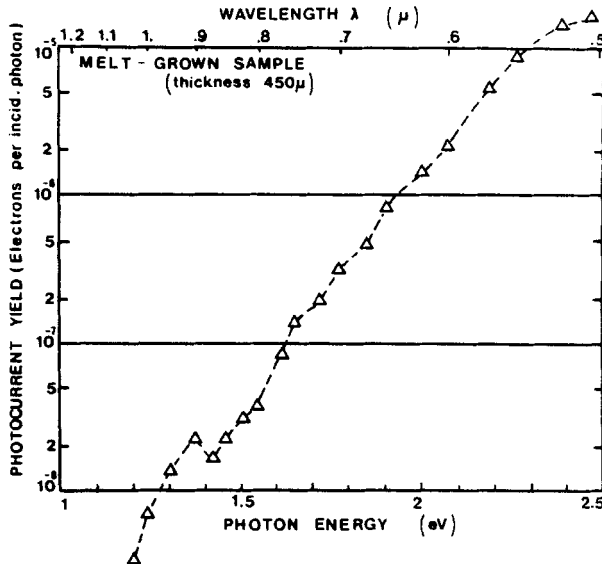


FIGURE 10 Spectral yield of photo-enhanced space-charge-limited current under forward injecting voltage of 500V.

## CONCLUSION

A fairly detailed characterization of the hole trap distribution in vapour-grown anthracene samples has been obtained. The techniques used previously in characterizing the electron traps in anthracene, have proved equally effective for the study of hole traps. Two main sets of hole traps, shallow and deep, were identified. The shallow set lies about 1 eV above the valence-band edge and is present with a density of  $\sim 10^{11} \text{ cm}^{-2}$ . The deep set lies in the range 1.8 - 2.3 eV above the valence-band edge and is of density  $\sim 5 \times 10^{12} \text{ cm}^{-3}$ . The cross section for direct optical excitation is  $\sim 5 \times 10^{-16}$  and  $\sim 5 \times 10^{-17} \text{ cm}^2$  for the shallow and deep sets of traps, respectively.

The trap density in the melt-grown crystals was found to be considerably lower ( $\sim 10^{11} \text{ cm}^{-3}$ ). As a result, their detailed characterization was not possible. All that could be definitely determined was the presence of one set of traps located higher than  $\sim 1.2 \text{ eV}$  above the valence-band edge. The nature and origin of the hole traps in either type of crystal is not known.

Studies of the spectral yield of the photocurrent arising from optical excitation out of the shallow set of traps in the vapour-grown samples yielded valuable information on the valence band structure of anthracene. The occurrence of a narrow peak near the threshold of the yield curve constitutes strong evidence for the existence of a narrow conducting sub-band at the top of the valence band of anthracene. The width of the peak—about 0.2 eV—is determined by the width of the sub-band on the one hand and by the spread in energy location of the shallow traps. Hence, the width of the sub-band can be at most 0.2 eV, probably less. Similar arguments indicate that the sub-band is separated from the much broader continuum of lower-lying conducting states by at most 0.2 eV. These findings are compatible with theoretical expectations<sup>4,6</sup> and with less detailed indications for the existence of such a sub-band obtained by other workers<sup>7-9</sup>. These workers attributed their photocurrent data to photoemission from the metal contact, an interpretation that we question. Further discussion of this point is published elsewhere.<sup>10</sup>

It appears that de-trapping of holes by photo-generated triplet excitons<sup>11</sup> is far less significant than in the case of electron traps.<sup>1</sup> Since the same types of crystals were used in studies of both the electron and hole photocurrents (triplet lifetime of about 5 msec), one concludes that the ratio of the cross section for triplet de-trapping and for direct photoexcitation is considerably smaller for hole than for electron traps.

## References

1. Many, A., Levinson, J. and Teucher, I, *Mol. Crystals* 5, 273 (1969).
2. Kepler, R. G. *Phys. Rev.* 119, 1226 (1960).

3. See, e.g., A. Many, Y. Goldstein and N. B. Grover, *Semiconductor Surfaces* (North-Holland Publishing Co., Amsterdam, 1965). p. 76.
4. Leblanc, O. H., Jr., *J. Chem. Phys.* **35**, 1275 (1961).
5. Hoesterey, D. C., and Leston, G. M., *J. Phys. Chem. Solids* **24**, 1609 (1963).
6. Silby, S., Jortner, J., Rice, S. A. and Vala, M. T., *J. Chem. Phys.* **42**, 733 (1965).
7. Williams, R. and Dresner, J., *J. Chem. Phys.* **46**, 2133 (1967).
8. Dresner, J., *Mol. Crystals and Liquid Crystals* **11**, 3, 307 (1970).
9. Vaubel, G. and Baessler, H., *Phys. Letters* **27A**, 328 (1968).
10. Levinson, J., Burshtein, Z. and Many, A., *Mol. Cryst. Liq. Cryst.*, in press.
11. Ern, V., Bouchrila, H., Fournery, J. and Delacote, G., *Solid State Comm.* **9**, 1201 (1971).